Non-equilibrium dynamic critical scaling of the quantum Ising chain

Michael Kolodrubetz[1], Bryan K. Clark[1,2], David A. Huse[1,2]

[1]*Department of Physics, Princeton University, Princeton,
NJ 08544, USA.* [2]*Princeton Center for Theoretical Science.*
(Dated: July 10, 2012)

We solve for the time-dependent finite-size scaling functions of the 1D transverse-field Ising chain during a linear-in-time ramp of the field through the quantum critical point. We then simulate Mott-insulating bosons in a tilted potential, an experimentally-studied system in the same equilibrium universality class, and demonstrate that universality holds for the dynamics as well. We find qualitatively athermal features of the scaling functions, such as negative spin correlations, and show that they should be robustly observable within present cold atom experiments.

The Kibble-Zurek (KZ) mechanism describes the dynamics of a system as it is ramped across a phase transition at a finite rate. Kibble first introduced this idea to model symmetry breaking during cooling of the early universe [1]. Later, Zurek showed that condensed matter systems exhibit similar behavior in the context of slowly ramping across the superfluid phase transition in liquid ^{4}He [2]. Both proposals looked at ramps from deep in the disordered phase to deep in the ordered phase. Historically, this has been the primary focus of research on the KZ mechanism (c.f.e. [3, 4]), although recent work has explored ramps that end at the critical point [5–7].

However, the scaling theory of the KZ mechanism applies more generally than these two limits. Near the quantum critical point (QCP), observables measured during the ramp are postulated to exhibit universal scaling forms [8, 9]. In this Letter we solve for the scaling functions of excess heat and equal-time spin correlations in the 1D transverse-field Ising (TFI) chain for two scaling directions – time t during the ramp and finite size L – and investigate the qualitative features of these observables. In many cases, the quantum dynamics of a closed non-integrable quantum system lead to a thermal state. In contrast, we show here that the spin correlation functions are qualitatively different from those of any thermal state. We also find a ramp protocol where the state at long time not only does not thermalize, but also does not dephase to the diagonal ("generalized Gibbs") ensemble. We provide evidence for the universality of the dynamics by using time-dependent matrix product states (tMPS) to simulate the experimentally-realizable, non-integrable model of Mott insulating bosons in a tilted potential [10, 11]. We see that the athermal features of the TFI chain are robust for small systems and discuss the prospects of seeing scaling collapse in present-day experiments.

Transverse-field Ising chain - The Hamiltonian for the TFI chain on an L-site 1D lattice is

$$H = -J \sum_{j=1}^{L} \left[(1-\lambda) s_j^x + s_j^z s_{j+1}^z \right], \qquad (1)$$

where λ is a tunable transverse magnetic field and $s^{x,z}$ are Pauli matrices with periodic boundary conditions ($s_1 = s_{L+1}$). We work in units where $\hbar = 1$ and $J = 1/2$. This model has a quantum phase transition (QPT) at $\lambda_c = 0$ [12]. In equilibrium, the system is in a disordered paramagnetic (PM) phase for $\lambda < 0$, while for $0 < \lambda < 2$, the system is in a ferromagnetic (FM) phase with two degenerate ordered ground states in the limit $L \to \infty$.

The Hamiltonian of the TFI chain can be diagonalized by applying a Jordan-Wigner transformation [12, 13]:

$$s_j^x = 1 - 2c_j^\dagger c_j, \quad s_j^z = -(c_j + c_j^\dagger) \prod_{m<j} s_m^x, \qquad (2)$$

where $c_j^\dagger$ creates a fermion at site j. As the Hamiltonian conserves fermion number modulo 2 and the ground state has an even number of fermions [13], we restrict ourselves to that subspace. Fourier transforming,

$$H = \sum_k \left[(1 - \lambda - \cos k) c_k^\dagger c_k + \frac{\sin k}{2} (c_k^\dagger c_{-k}^\dagger + c_{-k} c_k) \right]. \qquad (3)$$

This Hamiltonian can only excite fermions in momentum pairs $(k, -k)$, so we introduce a pseudo-spin σ corresponding to whether the $(k, -k)$ pair is filled ($\sigma^z = 1$) or unfilled ($\sigma^z = -1$). Then in the sector where all fermions are paired, which contains the ground state, $H = \sum_{k=0}^{\pi} H_k$, where

$$H_k = (1 - \lambda - \cos k) \sigma^z + (\sin k) \sigma^x . \qquad (4)$$

Note that H is a free-fermion Hamiltonian, so the TFI chain is integrable.

In a KZ ramp, λ is varied as a function of time near the critical point. For simplicity, we focus primarily on the case of a linear ramp, $\lambda(t) = vt$, where v is the ramp rate and the QCP is at $\lambda = t = 0$. The ramp begins at $t = -\infty$ deep in the disordered phase, where the wavefunction is initialized in the ground state of the instantaneous Hamiltonian $H(t = -\infty)$. For an infinite system, the Hamiltonian is gapless at the critical point. Therefore, it is impossible to ramp slowly enough through the

QCP to avoid creating excitations and to produce true long range order in the ordered phase.

Near the QCP, critical slowing down tells us that the characteristic time scale $\xi_t \sim \lambda^{-\nu z}$ becomes arbitrarily large, where ν and z are the (positive) correlation length and dynamic critical exponents respectively. Thus for a non-zero ramp rate, there exists a Kibble time, $-t_K$, at which the lowest momentum modes stop following the ramp adiabatically and become significantly excited. More explicitly,

$$
\begin{aligned}
|t_K| &= \xi_t(\lambda(|t_K|)) \sim |vt_K|^{-\nu z} \\
&\Rightarrow t_K \sim v^{-\nu z/(1+\nu z)} .
\end{aligned}
\tag{5}
$$

For the TFI chain $\nu = z = 1$, so $t_K \sim v^{-1/2}$. One can similarly define a length $\ell_K \sim t_K^{1/z}$ such that t_K and ℓ_K set the characteristic time and length scales for the Kibble-Zurek scaling forms [8, 9].

For a KZ ramp of the TFI chain, the wavefunction $|\psi(t)\rangle$ can be written as a product $|\psi(t)\rangle = \otimes_k |\Psi_k(t)\rangle$, where each mode evolves independently as

$$
\begin{aligned}
id|\Psi_k\rangle/dt &= H_k(t)|\Psi_k\rangle \\
&= [(1 - vt - \cos k)\sigma_k^z + (\sin k)\sigma_k^x]|\Psi_k\rangle .
\end{aligned}
\tag{6}
$$

The KZ scaling limit is defined as taking $v \to 0$ with τ, Λ, and κ constant [8, 9], where

$$
\begin{aligned}
\tau &\equiv tv^{1/2} \sim t/t_K \\
\Lambda &\equiv Lv^{1/2} \sim L/\ell_K \\
\kappa &\equiv kv^{-1/2} \sim k\ell_K \\
&= \frac{2\pi(n+1/2)}{\Lambda}.
\end{aligned}
\tag{7}
$$

Here $n = 0, 1, ..., (L/2) - 1$ indexes the modes. Note that $L \to \infty$ in the scaling limit, as $\ell_K \to \infty$ and Λ is constant. In this KZ scaling limit, eq. 6 simplifies to

$$
id\Psi_\kappa/d\tau = (-\tau\sigma_\kappa^z + \kappa\sigma_\kappa^x)\Psi_\kappa .
\tag{8}
$$

Each mode $\Psi_\kappa(\tau)$ in (8) has the form of a Landau-Zener (LZ) equation, which we solve in terms of parabolic cylinder functions [14]. Note that $\Psi_\kappa(\tau)$ is expressed solely in terms of the scaled variables τ and κ.

Observables - A crude measure of deviation from adiabaticity is the excess heat, defined as

$$
Q(t) = \sum_\kappa [\langle\Psi_\kappa(t)|H_\kappa(t)|\Psi_\kappa(t)\rangle - \langle\Psi_\kappa^0(t)|H_\kappa(t)|\Psi_\kappa^0(t)\rangle] ,
\tag{9}
$$

where $|\Psi_\kappa^0(t)\rangle$ is the instantaneous ground state of $H_\kappa(t)$. Defining excited state occupancy $p_\kappa^{\text{exc}} = 1 - |\langle\Psi_\kappa^0|\Psi_\kappa\rangle|^2$ and energy $E_\kappa^{\text{exc}} = 2v^{1/2}\sqrt{\tau^2 + \kappa^2}$, the scaled excess heat density is

$$
q(\tau, \Lambda) \equiv \frac{Q(t)}{vL}
$$

$$
= \frac{2}{\Lambda}\sum_\kappa p_\kappa^{\text{exc}}(\tau, \Lambda)\sqrt{\tau^2 + \kappa^2} .
\tag{10}
$$

For the equal-time s^z-s^z correlation function, we postulate a non-equilibrium scaling form, and check for scaling collapse. The correlation function is defined as $G(x) = \langle s_j^z s_{j+x}^z \rangle$, assuming translation invariance. In equilibrium, s^z has scaling dimension $1/8$, so the scaled correlation function is

$$
g(\tau, \Lambda, \chi) \equiv G(x, t, L, v)x^{1/4},
\tag{11}
$$

where $\chi \equiv xv^{1/2}$. We break up each site into a pair of Majorana fermions [12], such that the correlation function is the Pfaffian of a matrix whose elements are pairwise expectation values of the Majoranas [15]. We evaluate the Pfaffian numerically [16], and find that good scaling collapse occurs for small v (see fig. 1a).

During the initial part of the ramp ($\tau \ll -1$), the system is very nearly in equilibrium (figs. 2a, 1b). Deep on the FM side of the ramp ($\tau \gg 1$), LZ physics tells us that the excitation probability of mode κ is [14]

$$
p_\kappa^{\text{exc}} = \exp(-\pi\kappa^2) .
\tag{12}
$$

In between, at finite positive τ, the excitation probability for each mode – given by the LZ equation – oscillates as a function of scaled time before converging to (12). These oscillations show up in the excess heat (fig. 2a) and the correlation function (fig. 1b,c).

Finite-size effects enter by opening up a gap at the QCP. In the regime of small scaled size $\Lambda \lesssim 1$, the finite-size gap dominates, the system remains near the ground state, and the solution can be understood perturbatively. In the limit $\Lambda \to \infty$, on the other hand, finite-size effects vanish; we will refer to this as the thermodynamic limit of KZ scaling (KZ-TDL). Looking at the correlations right at the QCP (fig. 2b), we see the finite-size crossover from near-equilibrium power-law correlations for $\Lambda = 5$ to a non-equilibrium exponential decay of correlations for $\Lambda = 30$. Similarly, in fig. 2a we see that the scaled excess heat q crosses over from being small at $\Lambda = 5$, where the system is nearly adiabatic, to much larger values at larger Λ.

The TFI chain is integrable, so although a KZ ramp through the critical point creates excitations, the resulting excited states differ markedly from equilibrium thermal states at the same energies. From (12), we see that at long times the populations of modes with $\kappa^2 < (\log 2)/\pi$ are inverted, i.e. at a negative effective temperature. This leads to qualitatively athermal physics in the scaled correlation function, which goes substantially negative by $\tau = 5$ over a range of scaled distances, as can be seen in figs. 2c and 1c. This is qualitatively different from any thermal state, which would have a finite correlation length but never negative correlations. Similar behavior has been seen outside the scaling regime for both slow
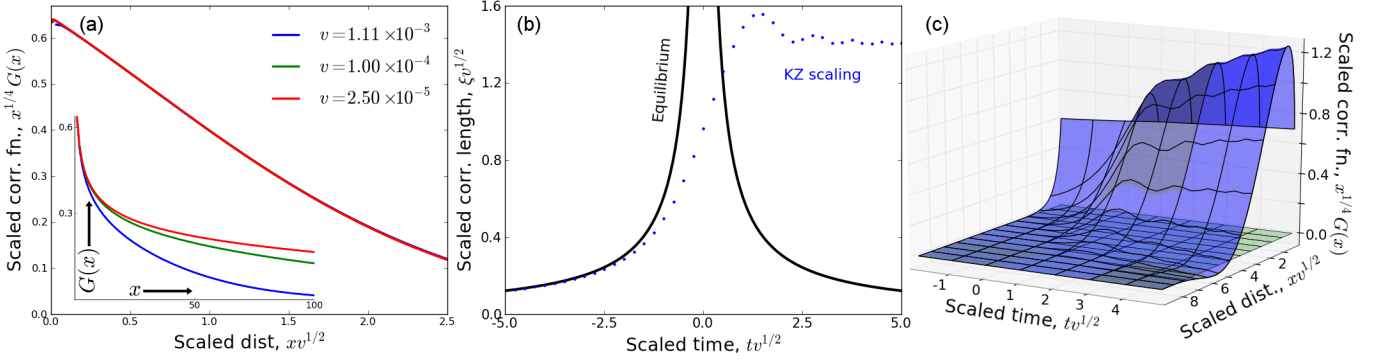
FIG. 1: (color online) (a) Spin-spin correlation function for the TFI chain for a ramp to the QCP ($t = 0$), showing scaling collapse for a wide range of slow ramp rates. The inset shows correlation functions prior to scaling. (b) Scaled correlation length and (c) correlation function as a function of scaled time (b,c) and distance (c) during the ramp. The KZ correlation length deviates from equilibrium near $tv^{1/2} = -2.5$ and remains finite at the QCP and beyond. We define the correlation length as $\xi v^{1/2} = \sqrt{\int_0^\infty g(\chi)\chi^2 d\chi / \int_0^\infty g(\chi)d\chi}$, where $\chi = xv^{1/2}$. All data in this figure are in the KZ thermodynamic limit, $Lv^{1/2} \gg 1$ (see text).

[17] and instantaneous [18] quenches of the TFI chain and the XY model [19].

Finally, we examine what happens formally as $\tau \to \infty$ while remaining in the scaling limit; in particular, does the system dephase? For comparison, if one were to stop the ramp at some value λ_f and wait a very long time, the phase differences between modes would increase to the point where the phases are essentially random; this process is known as dephasing. Dephasing in integrable systems is a well-studied problem, and it has been shown that, in the long time limit, the observables of the time-evolved pure state approach those of the generalized Gibbs ensemble (GGE, see ref. [20]), given by removing all phase information from each mode. Here we define the GGE at time τ as the dephased ensemble that one would approach upon freezing the current Hamiltonian and waiting a long time,

$$\rho_{\text{GGE}}(\tau) = \prod_\kappa \Big[(1 - p_\kappa^{\text{exc}}(\tau))|\Psi_\kappa^0(\tau)\rangle\langle\Psi_\kappa^0(\tau)| +$$
$$p_\kappa^{\text{exc}}(\tau)|\Psi_\kappa^1(\tau)\rangle\langle\Psi_\kappa^1(\tau)| \Big] , \quad (13)$$

where $|\Psi_\kappa^1(\tau)\rangle$ is the excited state of mode Hamiltonian H_κ. In the limit $\tau \to \infty$, the mode Hamiltonians asymptote to $H_\kappa \propto -\sigma_\kappa^z$, so the GGE approaches a fixed value with $|\Psi_\kappa^0\rangle \to |\uparrow\rangle$, $|\Psi_\kappa^1\rangle \to |\downarrow\rangle$, and $p_\kappa^{\text{exc}} \to e^{-\pi\kappa^2}$.

To see if $\tau \to \infty$ leads to dephasing, we consider the phase difference $\Delta\varphi$ between characteristic modes $\kappa = 0$ and $\kappa = 1$, since excitations are exponentially suppressed for $\kappa \gtrsim 1$. Starting from some time $\tau_i \gg 1$, after which the dynamics is effectively adiabatic, the energy difference ΔE and phase difference $\Delta\varphi$ are

$$\Delta E(\tau) = \sqrt{\tau^2 + 1} - \tau \approx \frac{1}{2\tau}$$
$$\Delta\varphi = \int_{\tau_i}^{\tau_f} \Delta E(\tau)d\tau \approx \frac{1}{2}\log(\tau_f/\tau_i) \quad (14)$$

Since $\Delta\varphi \to \infty$ as $\tau_f \to \infty$, the phase information between modes is lost in the long time limit, so the observables approach those of the GGE.

We note that, for non-linear ramps (say cubic ramps, $\lambda \sim t^3$), a similar scaling theory can be written down [8]. Then the above argument again holds, except now

$$\Delta\varphi \approx \int_{\tau_i}^{\tau_f} \frac{1}{2\tau^3} \to \text{const.} \quad (15)$$

as $\tau_f \to \infty$, implying that phase information remains, and the cubic ramp does not approach the GGE [21]. To summarize, both linear and cubic ramps exhibit athermal behavior, such as negative correlations, which come from the inversion of low-momentum modes, but only the linear ramp dephases to the GGE in the long time limit.

Tilted bosons - While the TFI chain is a beautiful theoretical model, it is difficult to realize in the lab. However, there have been a number of recent experimental advances with other, non-integrable models in the Ising universality class [11, 24, 25]. Here we focus on one, the Mott insulator in a tilted potential (MITP), realized experimentally in ref. [11]. The MITP consists of a one-dimensional lattice containing a Mott insulator with one boson per site. By adding a sufficiently large potential gradient (tilt) δ, the system undergoes a QPT from 1 boson per site to alternately 0 and 2 per site, creating dipoles on every other bond (see fig. 2a inset). This QCP is in the Ising universality class [10], and can be described by an effective spin Hamiltonian

$$H_{\text{eff}} = \mathcal{P}\left\{u\sum_l \left[\delta \frac{S_l^z + 1}{2} - S_l^x\right]\right\}\mathcal{P}, \quad (16)$$

where l labels the bonds, $S^{x,z}$ are Pauli matrices residing on the bonds, and $\mathcal{P}$ is a projector implementing the constraint that no two neighboring bonds are both spin
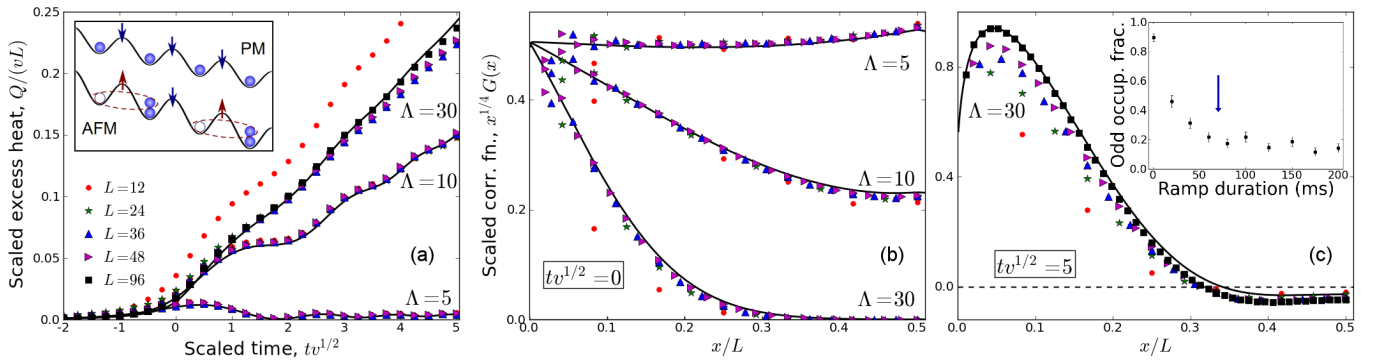
FIG. 2: (color online) Results of tMPS simulations for ramping the experimentally-realizable MITP model (see text), which is illustrated in the inset to (a). The data show scaling collapse of MITP (colored dots) to the scaling limit of the TFI chain (black lines) as a function of scaled time $\tau = tv^{1/2}$ (a), scaled system size $\Lambda = Lv^{1/2}$ (a,b), and scaled length x/L (b,c) [22]. We have checked that data for $\Lambda = 30$ is near the $\Lambda = \infty$ limit for the TFI model (not shown), although finite size effects can still be seen in (c). The arrow in the inset to (c) indicates the maximum ramp duration that produces athermal negative correlations in a twelve-site bosonic chain (data from Ref. 11, see [23] for details).

up. The energy scale is set by $u = \sqrt{2}w$, where w is the hopping energy of the lattice bosons; we work in units with $u = 1$. In analogy with the TFI chain, we define the parameters $\lambda = \delta_c - \delta$ and $v = \partial_t \lambda$ [22], where $\delta_c \cong -1.31$ is the location of the QCP [10]. The correlation function is given by $G(x) = (-1)^x \left(\langle S_j^z S_{j+x}^z \rangle - \langle S_j^z \rangle \langle S_{j+x}^z \rangle \right)$.

We simulate a linear ramp via tMPS, as described in ref. [7]. Fig. 2 shows calculated observables of the MITP model compared to the Ising scaling forms derived earlier. We see clear scaling collapse in all three scaling directions: ramp time t, system size L, and distance x. As expected, simulations do not collapse as well for smaller system sizes. While the dynamic range of the simulations is limited, and the scaling collapse for finite systems is imperfect, we consider our results to be strong numerical evidence for the postulated universality of KZ scaling for systems in the Ising universality class.

We note that, while scaling collapse for the system sizes considered is not perfect at $tv^{1/2} = 5$, the correlation function goes negative as predicted from the TFI scaling function. Therefore, the athermal physics of the KZ ramp is robust against small system sizes and the breaking of integrability, and is a qualitative feature of our model that should be visible experimentally. A major open question is whether such athermal behavior will manifest in KZ ramps near non-integrable QCPs, where the relatively short-time dynamics of the KZ ramp will be in competition with the long-time expectation of eigenstate thermalization [26].

Finally, we compare our time scales to the those of the real experimental system [11]. Using the experimental parameters $w \approx 10$ Hz and $U \approx 400$ Hz, where U is the on-site repulsion, we estimate the ramp rate necessary to see athermal negative spin correlation; our predicted ramp rates are shown in the inset to Fig. 2c compared to experimental data from Ref. 11. Clearly the necessary

ramp rates are well within the experimental range [23].

In conclusion, we have solved for the full Kibble-Zurek dynamic scaling forms of the one-dimensional transverse field Ising chain at zero temperature. We provided numerical evidence for the universality of these scaling relations via tMPS simulations of the MITP model. Finally, we determined that the relevant time scales for seeing these effects experimentally are within the reach of current technology. To see full scaling collapse the experimental system sizes need to be larger, but they should already be sufficient to see qualitatively similar athermal physics.

[1] T. Kibble, J Phys. A: Math. Gen. **9**, 1387 (1976).
[2] W. H. Zurek, Nature **317**, 505 (1985).
[3] B. Damski, Phys. Rev. Lett. **95**, 035701 (2005).
[4] A. del Campo, G. De Chiara, G. Morigi, M. B. Plenio, and A. Retzker, Phys. Rev. Lett. **105**, 075701 (2010).
[5] C. De Grandi, A. Polkovnikov, and A. W. Sandvik, Phys. Rev. B **84**, 224303 (2011).
[6] C. De Grandi, V. Gritsev, and A. Polkovnikov, Phys. Rev. B **81**, 012303 (2010).
[7] M. Kolodrubetz, D. Pekker, B. K. Clark, and K. Sengupta, Phys. Rev. B **85**, 100505 (2012).
[8] A. Chandran, A. Erez, S. S. Gubser, and S. L. Sondhi,

arXiv:1202.5277 (2012).

[9] S. Deng, G. Ortiz, and L. Viola, EPL (Europhysics Letters) **84**, 67008 (2008), ISSN 0295-5075.

[10] S. Sachdev, K. Sengupta, and S. M. Girvin, Phys. Rev. B **66**, 075128 (2002).

[11] J. Simon, W. S. Bakr, R. Ma, M. E. Tai, P. M. Preiss, and M. Greiner, Nature **472**, 307 (2011), ISSN 0028-0836.

[12] S. Sachdev, *Quantum Phase Transitions* (Cambridge University Press, 1999).

[13] J. Dziarmaga, Phys. Rev. Lett. **95**, 245701 (2005).

[14] C. Zener, Proceedings of the Royal Society of London A **137**, 696 (1932).

[15] E. Barouch and B. M. McCoy, Phys. Rev. A **3**, 786 (1971).

[16] We note that, in principle, the theory of Toeplitz determinants [27] can be used to analytically solve for the correlation function in the limit $x \gg 1$.

[17] L. Cincio, J. Dziarmaga, M. M. Rams, and W. H. Zurek, Phys. Rev. A **75**, 052321 (2007).

[18] K. Sengupta, S. Powell, and S. Sachdev, Phys. Rev. A **69**, 053616 (2004).

[19] R. W. Cherng and L. S. Levitov, Phys. Rev. A **73**, 043614 (2006).

[20] M. Rigol, V. Dunjko, V. Yurovsky, and M. Olshanii, Phys. Rev. Lett. **98**, 050405 (2007).

[21] We note two points about observing dephasing in practice. First, our arguments only hold when taking the long time limit while remaining near the QCP ($\lambda \ll 1$) to stay in the scaling regime. This limit is difficult to achieve, and is compounded by disorder, which becomes more important in the slow ramp, long time limit. Second, one must know the exact location of the QCP for the cubic ramp; a slight "miss" would allow one to linearize about the actual QCP. The slower the ramp, the more accurately one needs to know the QCP to see cubic scaling.

[22] There is an overall non-universal scaling between the TFI and MITP models, given empirically by $v_{\mathrm{MITP}} = 4.84 v_{\mathrm{TFI}}$, $G_{\mathrm{MITP}} = 0.196 G_{\mathrm{TFI}}$, and $t_{\mathrm{MITP}} = 0.557 t_{\mathrm{TFI}}$. All values in fig. 1 are those of the TFI chain, while fig. 2 gives those of the MITP model.

[23] Our analysis neglects the effect of disorder and open boundary conditions, which will need to be included to fully describe the Harvard experiment. See the supplemental information for brief analysis of open boundary conditions.

[24] J. Zhang, F. M. Cucchietti, C. M. Chandrashekar, M. Laforest, C. A. Ryan, M. Ditty, A. Hubbard, J. K. Gamble, and R. Laflamme, Phys. Rev. A **79**, 012305 (2009).

[25] K. Kim, S. Korenblit, R. Islam, E. E. Edwards, M.-S. Chang, C. Noh, H. Carmichael, G.-D. Lin, L.-M. Duan, C. C. J. Wang, et al., New Journal of Physics **13**, 105003 (2011), ISSN 1367-2630.

[26] M. Rigol, V. Dunjko, and M. Olshanii, Nature **452**, 854 (2008), ISSN 0028-0836.

[27] T. T. Wu, Phys. Rev. **149**, 380 (1966).

[28] T. D. Kühner, S. R. White, and H. Monien, Phys. Rev. B **61**, 12474 (2000).

Supplementary information for "Non-equilibrium dynamic critical scaling of the quantum Ising chain"

For theoretical simplicity, in the main text we have addressed the behavior of both the TFI chain and the MITP model with periodic boundary conditions. In the thermodynamic limit, boundary conditions have no effect on the bulk behavior. However, in experimental practice [11], the MITP model is realized in a finite (indeed, small) system with open boundary conditions. To better understand the experimental consequences of our work, we now address the KZ dynamics of the MITP model with open boundary conditions. We solve for the spin-spin correlation function $G(x)$ for the same criteria as in fig. 2 from the main text, with the results show in fig. 3.

Open boundary conditions (o.b.c.) in the MITP model differ from periodic boundary conditions (p.b.c.) only by the absence of the projector $\mathcal{P}$ on the ends of the chain, which in p.b.c. projects out configurations with up spins on both the first and last sites. As a result, on the ordered side of the phase transition, both the first and last sites will favor spin up over spin down due to the Zeeman field (see fig. 3d). This results in a large even/odd effect with regards to the system size: for odd size systems, there is no problem creating the staggered AFM state with up spins on each end, but for even size systems this ordering becomes frustrated. Note that a similar effect can be seen with p.b.c.: for L odd the AFM is frustrated.

An additional complication with o.b.c. is that, compared to the translationally invariant system with p.b.c., there is no unique way to define $G(x)$; due to the loss of translation invariance,

$$\langle S_j^z S_{j+x}^z \rangle - \langle S_j^z \rangle \langle S_{j+x}^z \rangle \neq \langle S_j^z S_{j+x}^z \rangle - \langle S^z \rangle^2 \ , \quad (17)$$

where $\langle S^z \rangle \equiv \frac{1}{L} \sum_j \langle S_j^z \rangle$. Choosing either side of (17) in defining $G(x)$ gives quantitatively different results. Similarly, including sites near the end of the chain in the definition of $G(x)$ introduces end effects whereas considering only spin correlations between sites in the middle third of the chain emphasizes the bulk behavior at the expense of throwing away data. The results we show in this supplement use the definition

$$G(x) \equiv (-1)^x \frac{1}{L-x} \sum_{j=1}^{L-x} \left[\langle S_j^z S_{j+x}^z \rangle - \langle S^z \rangle^2 \right] \ . \quad (18)$$

Empirically (data not shown), the various definitions of $G(x)$ that we described above gave quantitatively different, but qualitatively similar, results, that all approached the p.b.c. solution – as discussed below – in a similar manner.

The spin-spin correlations resulting from a KZ ramp of the MITP with o.b.c. are shown in fig. 3, panels a-c. The even/odd effects discussed above are apparent in a slow sweep (fig. 3a), with neither even nor odd
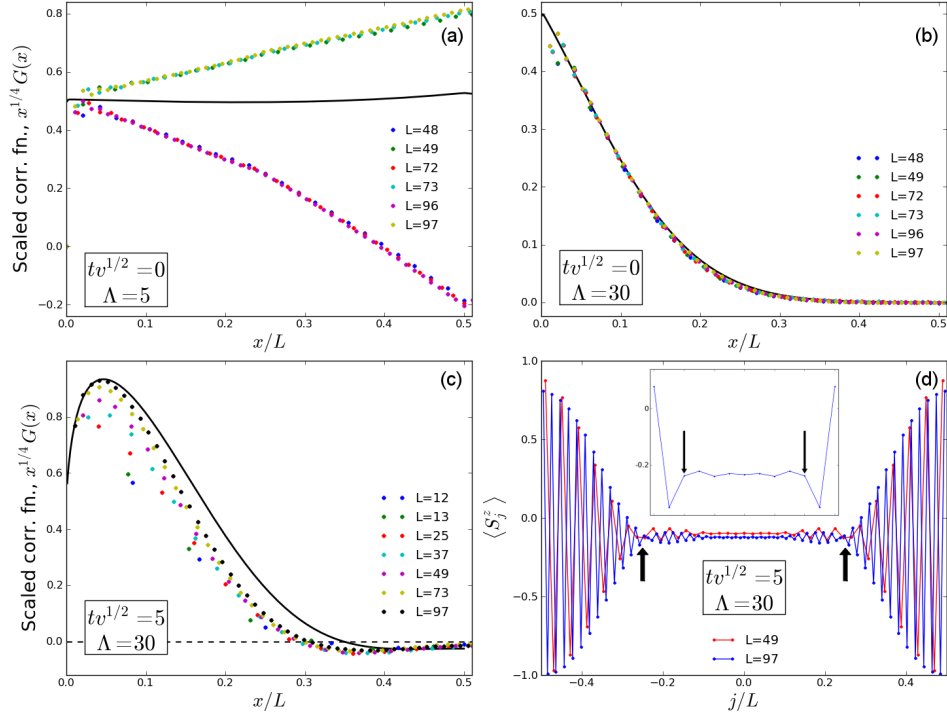
FIG. 3: (color online) (a-c) Spin-spin correlation function of the MITP model with open boundary conditions, compared to the TFI scaling function with p.b.c. (black lines). (d) z components of the individual spins, S_j^z, for the same parameters as (c) with $L = 97$, 49, and 13 (inset) sites, where j is the site index. Arrows indicate the $180°$ phase shift (AFM domain wall) that yields the negative correlations in (c).

size systems matching the p.b.c. solution. In general, matching between o.b.c. and p.b.c. solutions improves in the limit of fast sweeps (fig. 3b,c). This is not surprising, as finite size effects vanish in the KZ-TDL, so boundary conditions should have no effect in that limit. Note that fig. 3 shows scaled correlations as a function of scaled length x/L, and we see that the solutions match better at small distances $x \ll L$, where boundary effects are not important, as opposed to $x/L \sim 0.5$, where boundary effects are non-trivial.

Most importantly, the athermal negative correlations that we saw with p.b.c. exist with o.b.c. (fig. 3c), and therefore are robust with respect to both boundary conditions and small system size. In fact, o.b.c. enhances the ability to see negative correlations experimentally. As seen in fig. 3d, due to the absence of the end projector, the system breaks the $\mathbb{Z}_2$ Ising symmetry and selects the AFM with higher spin-up probability at the ends. By breaking the degeneracy of the ground states, the domain walls associated with negative correlations can be seen simply by measuring the expectation value of S_j^z for each site j, rather than measuring correlation functions. As expected from fig. 3c, for constant Λ these domain walls occur at a roughly constant value of j/L. This prediction, confirmed in fig. 3d, implies that the position of the domain wall relative to the edge of the sample is tunable by the ramp rate v.

Based on these observations, we estimate the ramp rates necessary to see athermal spin correlations at distance x equal to half the system size, using the definition of $G(x)$ from above. The results, shown in the inset to Fig. 2c in the main text for a twelve-site bosonic chain, indicate the the time scales necessary to see this phenomenon are already within experimental reach. However, we should note that for the smallest system shown in Ref. [11], a six-site bosonic chain, the negative correlations do not appear due to finite size effects. For any even length chain larger than six sites, these athermal correlations do robustly appear.

In conclusion, while open boundary conditions have a non-trivial effect on the scaling dynamics of the MITP model, these effects are diminished in the limit $Lv^{1/2} \gg 1$ or $x \ll L$. Crucially, the qualitatively athermal property of negative correlations survives for o.b.c. and small system size L. In fact, the breaking of the ground state degeneracy that occurs as a result of boundary conditions makes seeing these negative correlations easier experimentally, as domain walls in measurements of S^z. Therefore, we believe that many of the qualitative features of the TFI scaling functions should be experimentally accessible, while the quantitative scaling collapse will require larger system size or some mechanism to compensate for the open boundary conditions (c.f.e. [28]).